Beam Quality of High Power Vertical Cavity Surface Emitting Laser Single Device

Cui Jinjiang[1] Dong Ningning[1] Xu Jiangen[1] Xu Jie[2] Lin Tao[3]

[1] *Suzhou Institute of Biomedical-Engineering and Technology, Chinese Academy of Sciences, Suzhou, Jiangsu* 215163, *China*
[2] *Nanjing University of Science and Technology, Nanjing, Jiangsu* 210094, *China*
[3] *Jiangsu Province Institute for Medical Equipment Testing, Nanjing, Jiangsu* 210000, *China*

Abstract To research the beam quality of high power vertical cavity surface emitting lasers (VCSELs) singledevices, the impact of the factors such as the current, the aperture, the substrate thickness on the M^2 factor, the far field divergence angle, near field and far field intensity distributionsis analyzed. It′sconcluded that, the current density of active area tends to be uniform with the increasing current until the current gets crowded, which inducesall partsemitting and has a circular symmetric beam distribution. The beam quality factor will be smaller with the improved beam quality. On the other hand, with the increasing aperture size of the active region, the lasing intensitydistribution becomes more uneven. While, beam quality will be worse with the increasing aperture size. For the effect of substrate thickness on the beam quality, all the factorsare considered, the optimum substrate thickness is about 100 μm. In order to obtain high power and high beam quality for the VCSELs single device, the oxidation diameter of 650 μm and P side electrode diameter of 580 μm are chosen, which can realize the uniform distribution of current density in the active region and the effective limits on current. This study provides a basis for looking for an effective method to improve the beam quality.

Key words lasers; vertical cavity surface emitting laser; single device; beam quality
OCIS codes 140.2020;140.7260;230.3670

垂直腔面发射半导体激光器单管的光束质量研究

崔锦江[1] 董宁宁[1] 徐建根[1] 许 杰[2] 林 涛[3]

[1] 中国科学院苏州生物医学工程技术研究所，江苏 苏州 215163
[2] 南京理工大学，江苏 南京 210094
[3] 江苏省医疗器械检验所，江苏 南京 210000

摘要 研究了大功率底发射垂直腔面发射激光器(VCSEL)单管器件光束质量，分析了电流、出光孔径、衬底厚度等因素对 M^2 因子、远场发散角、近场及远场光强分布等的影响。使用有限元的方法对不同电极及不同氧化孔径时有源区中电流密度的分布进行了计算，为了获得高功率、高光束质量的 VCSEL 器件，选择氧化孔径为 650 μm 以及 P 面电极直径为 580 μm，在对电流进行有效限制的同时实现了有源区中电流密度的均匀分布，从而抑制远场光斑中边模的产生，改善了光束质量。

关键词 激光器；垂直腔面发射激光器；单管器件；光束质量
中图分类号 TN248.4 **文献标识码** A
doi: 10.3788/CJL201542.s102007

1 Introduction

Recently vertical cavity surface emitting lasers (VCSELs) have emerged as attractive light sources for a

---

收稿日期: 2015-01-13; **收到修改稿日期**: 2015-03-04

基金项目: 江苏省自然科学基金(BK2012188)、江苏省产学研联合创新项目(BY2013034)、苏州市医疗器械与新医药专项(ZXY2013005)、苏州市医疗器械与新医药专项(ZXY201429)、吉林省与中国科学院省院合作项目(2014SYHZ0005)

作者简介: 崔锦江(1981—)，女，副研究员，主要从事半导体光电子器件方面的研究。E-mail: cuijj@sibet.ac.cn variety of applications, owing to the native advantages over edge emitting lasers like buried active regions, distributed reflectivities and simple inexpensive mounting. Nowadays, VCSELs with small diameter (less than 20 μm) and low output power of a few milliwatts have been widely used in optical communications, scanning and massive parallel optical interconnections. The applications in free space communication, laser pumping and material treatment are showing a growing market for high power diode lasers[1-3].

With the development of the epitaxial material quality and device technology, the high power VCSELs reached watt level become a worldwide research hotspot. At the same time, people have put forward higher requirements on the beam quality. It should improve the power density of the lasers, and meet with the coupling efficiency of optical fiber and the requirements for high efficiency solid laser pumping[4-7].

In this paper, the beam quality of high power VCSELs single devices is researched. The analysis of the impact of the factors such as the current, the aperture, the substrate thickness on the M^2 factor, the far field divergence angle, the near field and far field intensity distributions are given. This study provides a basis for looking for an effective method to improve the beam quality.

2 Device structure and process

Figure 1 illustrates the configuration of the sample structure used in this work. The multi-layer system is grown by metal organic chemical vapor deposition (MOCVD) epitaxy on an n-GaAs substrate. The inner cavity consists of three 8 nm-thick $In_{0.2}Ga_{0.8}As$ quantum wells embedded in 10 nm-thick GaAs barriers. Two $Al_xGa_{1-x}As$ cladding layers are introduced on both sides of the active region to improve longitudinal carrier confinement and to make the cavity one wavelength. The carbon-doped p-type distributed Bragg reflector (DBR) consists of 30 pairs of $Al_{0.9}Ga_{0.1}As$/GaAs with graded interface to reduce series resistance. The bottom Bragg reflector consists of 28 pairs silicon-doped $Al_{0.9}Ga_{0.1}As$/GaAs quarter-wavelength layer pairs. There is a 30 nm-thick AlAs layer located between the active region and the top p-type mirror, which is to be oxidized and converted to Al_xO_y as the current confinement layer. The top 40 nm GaAs contact layer is doped to a concentration of $1\times10^9/cm^2$ to achieve a good ohmic contact.

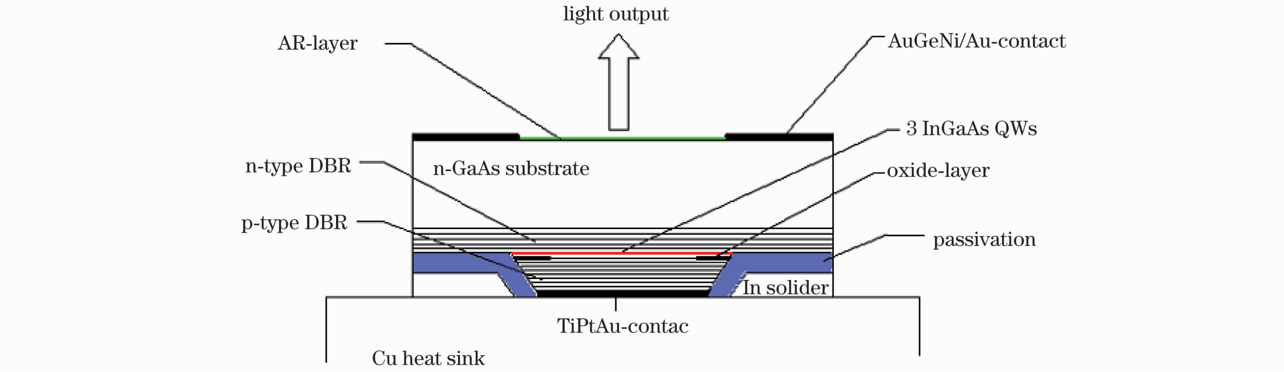

Fig. 1 Structure of bottom-emitting VCSEL

Mesa is wet chemically etched with sulphuric acid down to the depth of the AlAs layer. The AlAs layer is laterally oxidized for 30 minutes at 420 ℃ under nitrogen gas bubbled through water at 90 ℃ to form the current apertures with oxidation depths from 20 μm to 30 μm. A SiO_2 passivation layer is deposited on the mesa to avoid short circuits when soldering the device on heat sink. After selective etching of a circular SiO_2 film, TiPtAu is evaporated on the mesa by using electron beam deposition. Before depositing an antireflection (AR) coating of HfO_2, the substrate is thinned and polished to a thickness of 150 μm in order to reduce absorption losses. The emission window is then formed with alignment technique on double-face, which is surrounded by large-area AuGeNi/Au contacts. The whole chip is annealed at 420 ℃ in nitrogen environment condition for 60 seconds. Array devices are cleaved and then soldered junctiondown with AuSn-solder on a metallized diamond heat spreader. The diamond heat spreader is attached with In paste on a copper submount.

3 Analysis of beam quality

3.1 Effect of current on the laser beam quality

We fabricated a 300 μm aperture-size single device follow the methods above. The beam quality parameters at different working currents are measured using "the lens transformation method"[8]. Fig. 2 describes the relation between the beam radius and beam propagation distance at different currents. The beam radius $W(Z)$ and the propagation distance Z is brought into the Gauss formula, which describes the beam propagation as[9]

$$W(Z) = W_0\sqrt{1+\left[\frac{(Z-Z_0)\lambda M^2}{\pi W_0^2}\right]^2}, \tag{1}$$

where W_0 and Z_0 are the radius and the propagation distance of the beam waist in the Gaussian beam separately, λ is the wavelength of the VCSEL. The M^2 factors are 66, 58, 44, 53 separately at the current of 900, 1500, 3000, 6000 mA through the Gauss fitting. Fig. 3 is the far field distribution of 300 μm-aperture-size device at different currents.

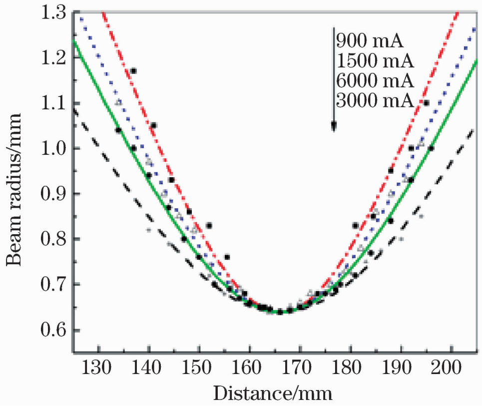

Fig. 2 Relationship between beam radius and propagation distance at different currents

At a low inject current, there is only the edge part emitting because of the large active-area, which induces a poor beam quality and annular beam distribution. With the current increasing, the current density of active area tends to be uniform, which induces all parts emitting and has a circular symmetric beam distribution. The beam quality factor will be smaller with the improvement of the beam quality. While, the current is easily to get crowded at the active region with the inject current increasing, which will induce a destruction of the current distribution in the active region and a worse beam quality[10].

3.2 Influence of output aperture size on beam quality

Figure. 4 is the far field distribution(simulated by Matlab) of the single devices with the aperture size of 200, 300, 400 μm at the same inject current of 3 A. As shown in Fig. 4, the current distribution is more uniform with a small aperture size for bottom-emitting VCSELs. The current density of edge area of the active region is similar to the current density of the center area. It means the whole output window emitting. The beam distribution is similar to the Gauss model at threshold current. The far field beam is central symmetry, with a high light intensity in center and the beam divergence angle less than 15°. With the aperture size of the active region increasing, the lasing intensity distribution becomes more uneven. The region with high injected carrier concentration has strong emitting, which induces uneven beam distribution. Beam quality becomes worse with the aperture size increasing.

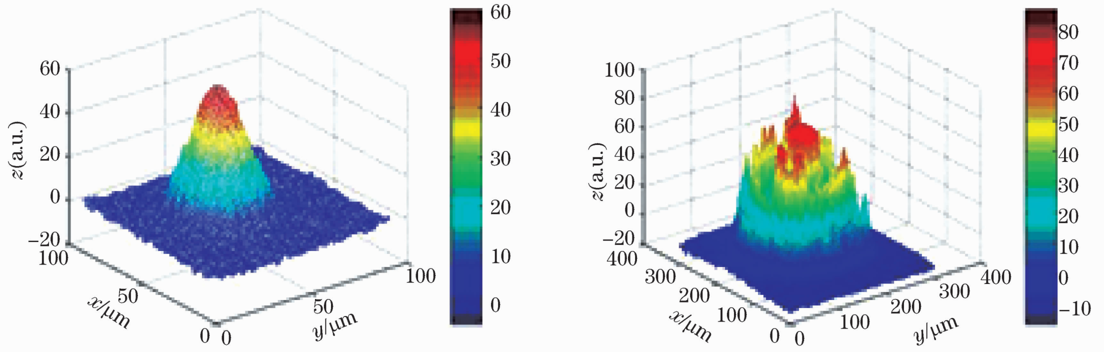

(a) $l=1.0$ A (b) $l=1.5$ A

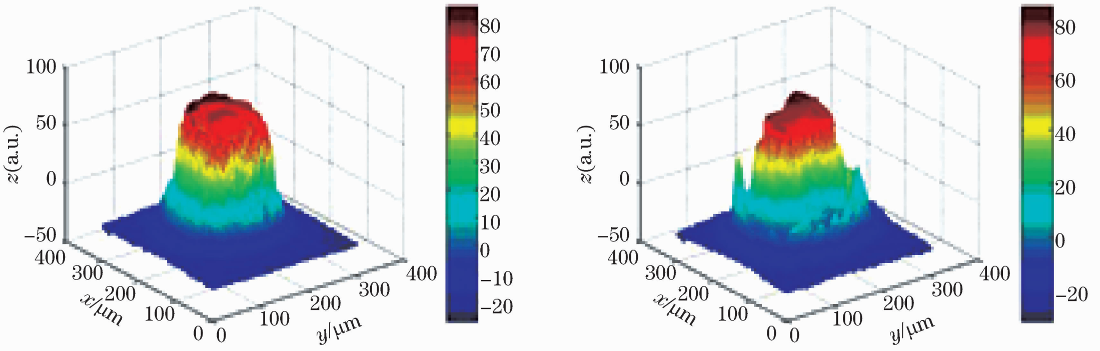

(c) $l=2.0$ A (d) $l=3.0$ A

Fig. 3 Far field distribution of 300 μm-aperture-size device at different currents

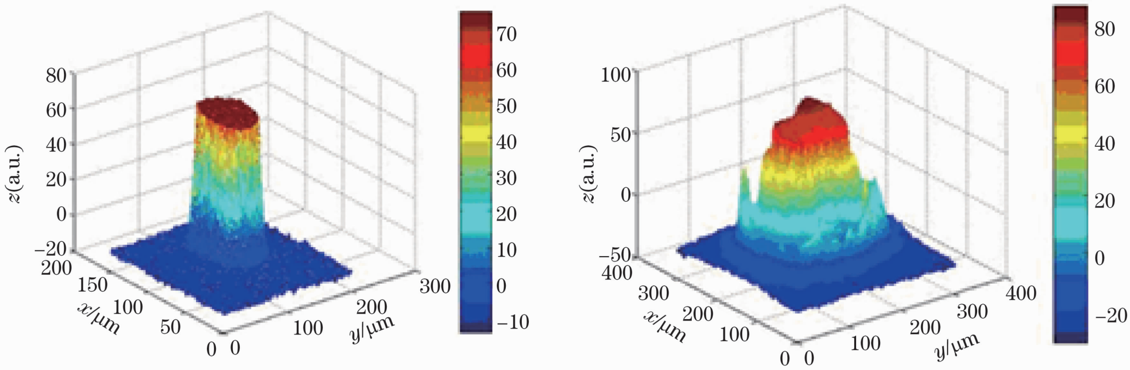

(a) diameter of 200 μm (b) diameter of 300 μm

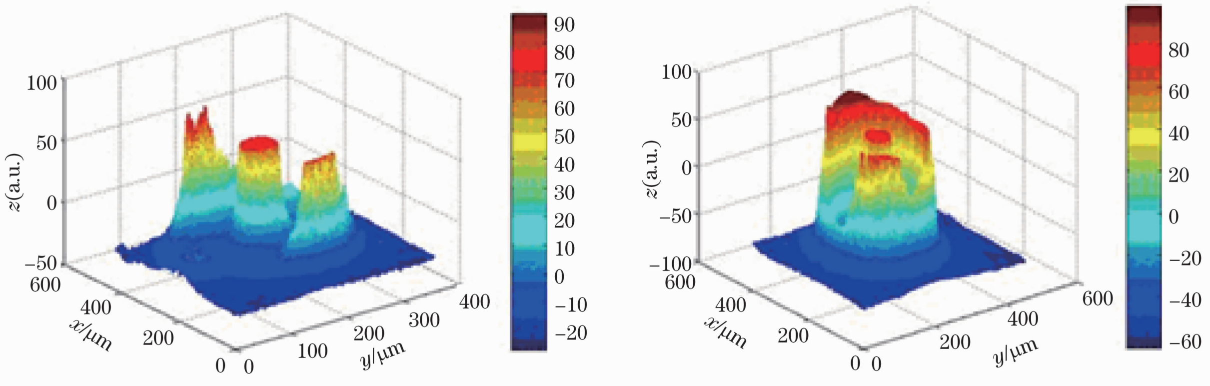

(c) diameter of 400 μm (d) diameter of 500 μm

Fig. 4 Far field distribution with different parameters at the current of 3 A

3.3 Effect of substrate thickness on the beam quality

The relationship between GaAs substrate thickness and the distribution of the current density in the active region is calculated using the ANSYS analysis software. The change of current density distribution in the active region with the substrate thickness of the device with 150 μm radius of the active region and 0.8 Ω series resistance is shown in Fig. 5. As shown in the figure, the current density of the central area will increase with the thickness of the substrate increasing. The current density distribution of the active region is relatively uniform when the substrate thickness is more than 100 μm. The substrate thickness should not be too thick considering the loss in the substrate. Considering all the factors, the optimum substrate thickness is about 100 μm.

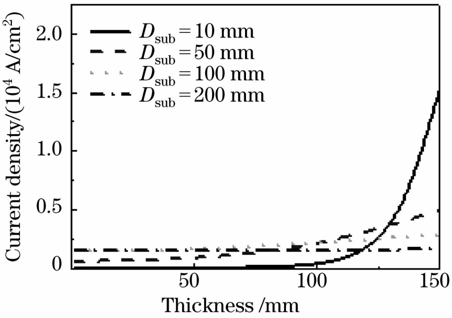

Fig. 5 Simulation of the relationship between current density of the active region and thickness of the substrate

3.4 Improvement of the far field divergence angle

As shown in Fig. 4, the aperture size of the output window is increased to realize high output power. The ununiform current density distribution in the large active region will induce strong side mode in the far field. In order to obtain high output power with reduced side mode and the far field angle, we calculate and analysis the current density distribution in the active region of the large aperture size device.

The calculation results are shown in Fig. 6, which describes the current density distributions of the active region with 650 μm-diameter and 580 μm-diameter of P-side electrode at different oxidation diameters, respectively.

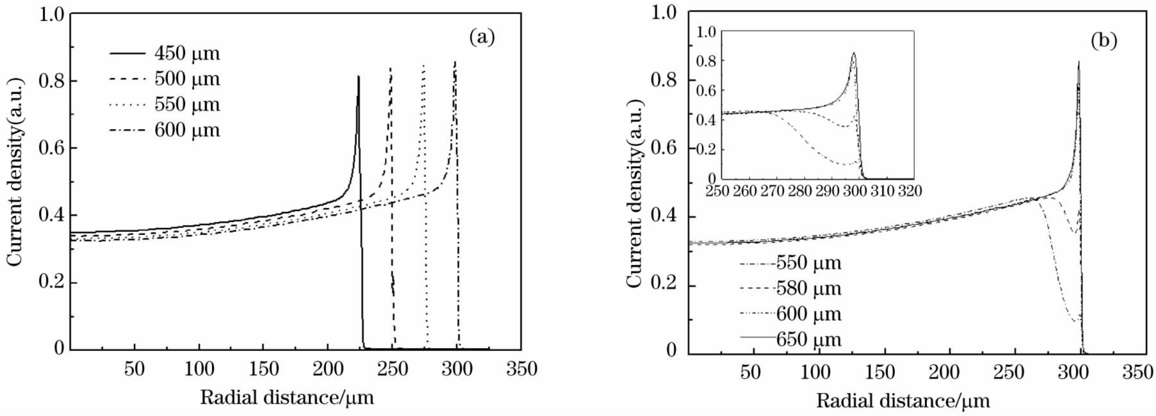

Fig. 6 (a) Simulation of the current density distribution of the active region with 650 μm-diameter P-side electrode at different oxidation diameters; (b) current density distribution of the active region with 580 μm-diameter of P-side electrode at different oxidation diameters

The diameter of the active region is determined by the oxidation aperture size. The distribution of the current density in the active region is determined by P-side electrode diameter and the oxidation diameter. As in Fig. 6, when the P-side electrode diameter is less than the oxidation diameter, the distribution of the current density in the active region is determined by both of them. The effect of the oxidation diameter on the current distribution decreases with the P-side electrode diameter decreasing. When the P -side electrode diameter is much smaller than the oxidation aperture, the distribution of the current density is only determined by the diameter of the P-side electrode.

According to the simulation results in Fig. 6(b), we choose the oxidation diameter of 650 μm and P side electrode diameter of 580 μm, which can realize the uniform distribution of current density in the active region and have the current effectively limited. So the generation of side mode in far field spot is suppressed.

Figure 7 describes the far field distribution of the device with the electrode diameter of 650 μm and 580 μm working at 4 A current. For the device with the electrode diameter of 650 μm, there is strong side mode appeared in the far field distribution at the working current of 1, 2, 4 A. The far field divergence angle (FWHM) is about 30°. This is due to the high current density of the edge of oxidation aperture induce the higher-order transverse mode emitting. This far field energy distribution is very unfavorable to optical fiber coupling. Fig. 7(b) is the far field distribution of the device with 580 μm electrode diameter. The far field divergence angle reduces to about 15°. The uniform distribution of current density in the active area makes the high order transverse mode of the oxide aperture edge restrain effectively. So the device worked with relatively low order mode and Gauss type distribution in the far field.

The circular symmetric light with small divergence angle can be coupled into the fiber use simple collimation focusing device and applied widespread.

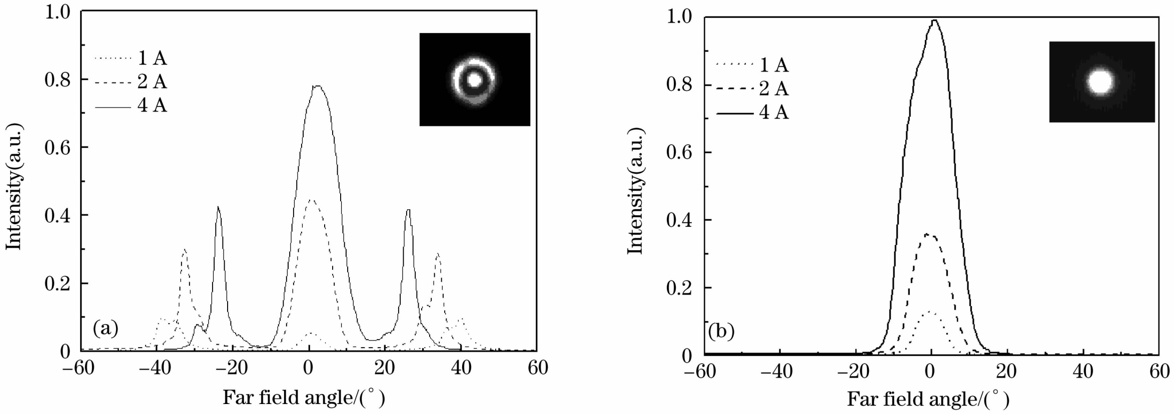

Fig. 7　Far field distribution of the devices with (a) 650 μm and (b) 580 μm P-side electrode diameter at the working current of 1 A,2 A and 4 A

Figure 8 is the power-current curves of devices with electrode diameter of 650 μm and 580 μm. The threshold current of the 650 μm devices is slightly lower than the threshold current of 580 μm devices. Because the high order mode will emit at a low current, the oxidation aperture edge still has high order mode even at a high current density for the 650 μm device.

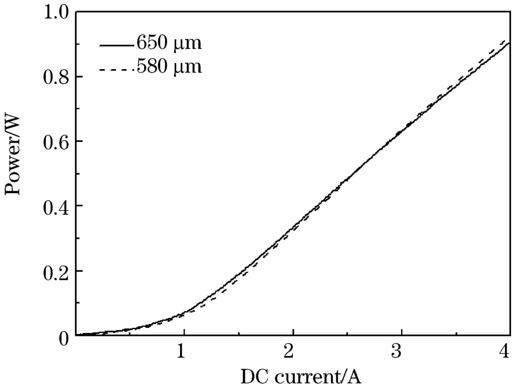

Fig. 8　Output power of the device with the aperture size of 650 μm and 580 μm

650 μm device has a higher output power than 580 μm device at a low current region ($I \leqslant 2.5$ A) due to

the existence of higher order mode. The highest output power of 580 μm device is higher than the 650 μm device. This may be due to the aggregation effect induced by the high current density at the oxidized aperture edge of the 650 μm device. The increasing scattering loss is not conducive to heat dissipation[11-12].

4 Conclusion

The beam quality of high power VCSELs single devices is researched. The analysis of the impact of the factors such as the current, the aperture, the substrate thickness on the M^2 factor, the far field divergence angle, the near field and far field intensity distributions is given. The distribution of current density in the active region is calculated at different electrodes and different oxidation aperture sizes using the finite element method. In order to obtain high power and high beam quality for the VCSELs single device, the oxidation diameter of 650 μm and P side electrode diameter of 580 μm are chosen, which can realize the uniform distribution of current density in the active region and the effective limits on current. As a result, the generation of side mode in far field distribution is suppressed. The beam quality is improved also. This study provides a basis for looking for an effective method to improve the beam quality.

References

1 Ma Jianli, Hao Yongqin, Zhong Jingchang, *et al*.. Study on stability of selective oxidation in vertical cavity surface emitting laser[J]. Chinese J Lasers, 2007, 34(8): 1055－1058.
马建立，郝永芹，钟景昌，等，垂直腔面发射激光器中选择性氧化工艺稳定性研究，[J]. 中国激光，2007, 34(8): 1055－1058.

2 M Grabherr, B Weigl, G Reiner, *et al*.. High power top-surface emitting oxide confined vertical-cavity laser diodes[J]. Electron Lett, 1996, 32(18): 1723－1724.

3 Van Leeuwen R, Xiong Y, Watkins L S, *et al*.. High power 808 nm VCSEL arrays for pumping of compact pulsed high energy Nd:YAG lasers operating at 946 nm and 1064 nm for blue and UV light generation[C]. SPIE, 2011, 912: 79120Z.

4 Van Leeuwen R, Xiong Y, Seurin J F, *et al*.. High-power vertical-cavity surface-emitting lasers for diode pumped solidstate lasers[C]. SPIE, 2012, 8381: 83810I.

5 Hao Y, Ma J, Yan C, *et al*.. A fundamental mode Nd:$GdVO_4$ laser pumped by a large aperture 808 nm VCSEL[J]. Laser Phys Lett, 2013, 10 (5) : 055003.

6 Chow W W, Choquette K D, Crawford M H, *et al*.. Design, fabrication, and performance of infrared and visible verticalcavity surface-emitting lasers[J]. IEEE J Quan Elec, 1997, 33(10): 1810－1824.

7 Cui Jinjiang, Ning Yongqiang, Jiang Chenyu, *et al*., Beam quality of high power vertical-cavity bottom-emitting semiconductor lasers[J]. Chinese J Lasers, 2011, 38(1): 0102002.
崔锦江，宁永强，姜琛昱，等，大功率垂直腔底发射半导体激光器的光束质量，[J]. 中国激光，2011, 38(1): 0102002.

8 International Organization for Standardization, Lasers and Laser-Related Equipment. Test Methods for Laser Beam Parameters, Beam Widths, Divergence Angle and Beam Propagation Factor[S]. ISO 11146, 1999.

9 Zhou Bingkun, Gao Yizhi, Chen Chourong, *et al*.. Laser Principle[M]. 4th edition. Beijing: National Defence Industry Press, 2000: 75.
周炳坤，高以智，陈倜嵘，等，激光原理[M]. 第 4 版. 北京：国防工业出版社，2000: 75.

10 Eric R Hegblom, Near M Margalit, Brian J Thibeault, *et al*.. Current spreading in apertured vertical cavity lasers[C]. SPIE, 2003: 176－180.

11 Hardley G R, W arren M E, Choquet te K D, *et al*.. Comprehensive numerical modeling of vertical cavity surface emitting lasers[J]. IEEE Journal of Quantum Electronics, 1996, 32 (4): 607－616.

12 Craig Angelos, Steven Hinckley, Rainer Michalzik, *et al*.. Simulation of current spreading in bottom-emitting vertical cavity surface emitting lasers for high power operation[C]. SPIE, 2004, 5277: 261－272.

栏目编辑： 史 敏